

Characterization of the fabrication process of Nb/Al–AlN_x/Nb tunnel junctions with low $R_n A$ values up to $1 \Omega \mu\text{m}^2$

N N Iosad¹, A B Ermakov², F E Meijer¹, B D Jackson³
and T M Klapwijk¹

¹ Department of Applied Physics (DIMES), Delft University of Technology, Lorentzweg 1, 2628 CJ Delft, The Netherlands

² Institute of Radioelectronics Russian Academy of Sciences, Mokhovaya 11, 103907, GSP-3, Moscow, Russia

³ Space Research Organization of the Netherlands, PO Box 800, 9700 AV Groningen, The Netherlands

E-mail: iosad@dimes.tudelft.nl and n.iosad@tnw.tudelft.nl

Received 5 February 2002

Published 3 May 2002

Online at stacks.iop.org/SUST/15/945

Abstract

We discuss and characterize the fabrication process of superconductor–insulator–superconductor (SIS) junctions based on a Nb/Al–AlN_x/Nb tri-layer. Utilization of the AlN_x tunnel barrier, produced by Al nitridation in a nitrogen glow discharge, enables us to produce high-quality SIS junctions with low $R_n A$ values (a product of junction resistance and area). We characterize the tunnel barrier formation and investigate the correlation of plasma characteristics and junction properties. The experiment shows that an increase in nitridation time and applied power results in an increase in junction resistance, while variation in nitrogen pressure has almost no influence on the junction characteristics. Analysing the correlation of junction resistance and plasma properties, it is concluded that the mechanism of tunnel barrier formation is based on nitrogen implantation into the Al layer with subsequent diffusion of nitrogen, stimulated by plasma heating.

1. Introduction

Pushing the operation of superconductor–insulator–superconductor (SIS) heterodyne mixers towards THz frequencies requires strip lines with low losses at these frequencies and high-quality SIS junctions with lower $R_n A$ values and a higher gap voltage compared to the SIS junctions based on a Nb/Al–AlO_x/Nb tri-layer [1–10]. Moreover, the utilization of SIS junctions with low $R_n A$ values allows us to design SIS mixers with lower noise temperatures and broader bandwidths. It has been shown that SIS junctions with the AlN_x tunnel barriers are superior to the AlO_x based tunnel junctions in these respects [5]. This method employs radio-frequency (rf) glow discharge in a nitrogen atmosphere for AlN_x tunnel barrier production [10].

The study of metal surface nitridation in a glow discharge was begun almost a century ago. Many different technological parameters have been identified as key parameters: metal temperature, glow-discharge type, the energy spectrum of bombarding ions and fast neutrals, gas composition, etc [11]. A successful method of AlN_x tunnel barrier growth, based on this principle, has been implemented by Shiota *et al* [12] in Nb/Al–AlN_x/Nb SIS junctions. Furthermore, this process has been studied in greater detail and compared with the Nb/Al–AlO_x/Nb process by Dolata *et al* [13]. However, this process fails to produce the high-quality SIS junctions with low $R_n A$ values [14]. This is due to the fact that the substrate located on a driven electrode is exposed to a very energetic and intense flux of ions during Al layer nitridation. Nitrogen ions not only perform nitridation of the Al layer, but also damage the

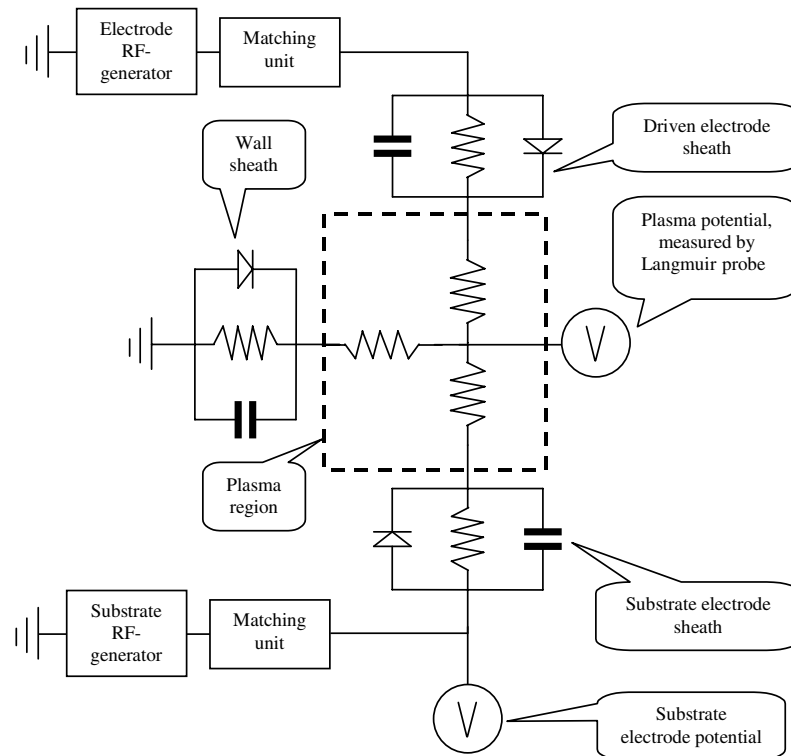


Figure 1. Electrical model for experimental system.

growing AlN_x layer [15]. A breakthrough has been achieved by Bumble *et al* [10]. They proposed to attach a substrate to a grounded electrode located parallel to a driven electrode. This allows a substantial reduction of the density and energy of bombarding ions. A properly designed system with a capacitively coupled driven electrode allows us to achieve the plasma potential almost equal to the floating potential [16]. In this case the bombarding ions activate the surface reaction without damaging the surface [15]. As it has been reported by Bumble *et al*, the chemical reaction dynamics of AlN_x tunnel barrier formation in their homemade vacuum system is not yet understood [10]. Therefore we focus on the characterization of the AlN_x tunnel barrier formation and the correlation of plasma characteristics with junction properties.

2. Experimental details

The junctions are produced in a Nordiko-2000 sputtering system with a base pressure of 4×10^{-5} Pa. This sputtering machine is equipped with a cryopump and a throttling valve, which together determine the process pressure, while the injection of Ar and N_2 gases is controlled by flow meters. All films are deposited by 3 inch Nordiko dc magnetrons at a maximum substrate–target distance for this system (8 cm) to achieve maximum uniformity of the layers. Wafers are fixed to the copper chucks, maintained at 20°C with diffusion pump oil to stabilize the substrate temperature.

Following the concept of minimization of the energy and intensity of the ion flux bombarding the Al surface during a process of nitridation, we have designed the following system. The driven electrode consists of the 4 inch Nordiko magnetron sputtering source with removed magnets. In other words,

the removal of magnets converted the sputtering source into an rf diode sputtering system. Taking into account that a sputtering of a target material will take place in any case, an Al target 99.99% pure was installed in this source. The target size is a triad between two contradicting factors: the target area has to be maximized to produce maximum uniformity of the ion flux towards the substrate surface, but on the other hand minimization on the target area results in a reduction of the plasma potential [15]. The latter consideration is fulfilled almost automatically since plasma non-confined by the magnetic trap is in contact with an area in the sputtering chamber which is much bigger than the cathode area. The electrode is connected to the rf generator via the Nordiko matching unit providing the capacitive coupling of plasma.

The substrate chuck is not grounded in our system and remains permanently connected to a matching unit and rf generator. This circumstance results in an additional issue of concern. An equivalent electric circuit is illustrated in figure 1. Various types of resonance may occur in this system. For example, a very high negative substrate bias of a substrate chuck may occur in this type of system, due to the series resonance between an inductive tuning network and a capacitive substrate sheath [17, 18]. We have investigated these factors carefully by manually changing the substrate matching unit impedance and measuring the substrate potential. The impedance of the substrate matching unit has been selected to avoid all these possible resonances.

The Langmuir probe, manufactured by Scientific Instruments, is employed for plasma characterization. The probe is located 2 cm above the centre of the substrate chuck. The flux of nitrogen ions bombarding the substrate during the nitridation procedure is characterized by two key

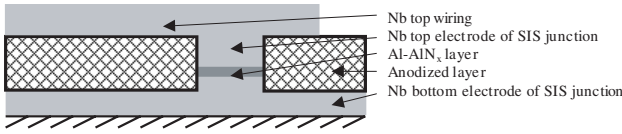


Figure 2. Cross-sectional view of an SIS junction produced by the selective niobium anodization process.

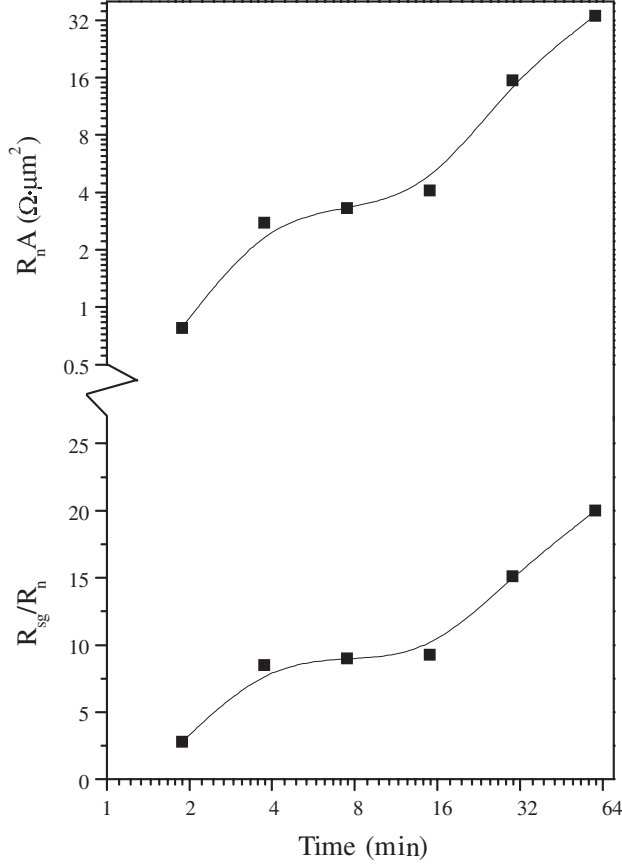


Figure 3. Junction properties versus nitridation time. Nitrogen pressure during Al layer nitridation is kept at 50 mTorr for all data points. Applied power during Al layer nitridation is kept at 30 W for all data points.

parameters: the voltage drop across the substrate sheath (V_{sh}), measured as a difference between the substrate and plasma potentials, and the ion current density injected into the sheath (J_i). The characterization of the plasma properties by the Langmuir probe revealed that V_{sh} values are very close to the plasma floating potential, indicating that the developed system produces the least possible plasma potential.

The tunnel junctions are produced by the selective niobium anodization process (SNAP) [19]. This process provides the fastest and the easiest way of junction production. A cross section of an SIS junction produced by the SNAP process is illustrated in figure 2. The production process consists of three steps:

- (1) a Nb/Al–AlN_x/Nb tri-layer is deposited in one run on a Si wafer;
- (2) a photoresist mask is formed to define 10 μm^2 junctions—a subsequent anodization up to 80 V of the top Nb layer and Al–AlN_x layers completes the junction formation;

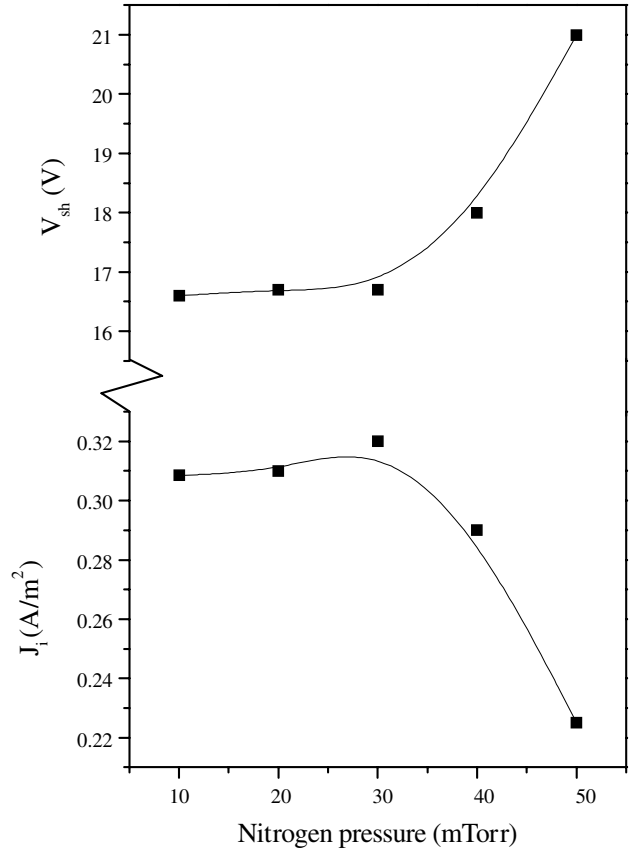


Figure 4. Voltage drop across the substrate sheath and ion current density injected into the sheath. Applied power is kept at 30 W for all data points.

- (3) top wiring, consisting of Nb and Au layers, is sputtered via a lift-off photoresist mask.

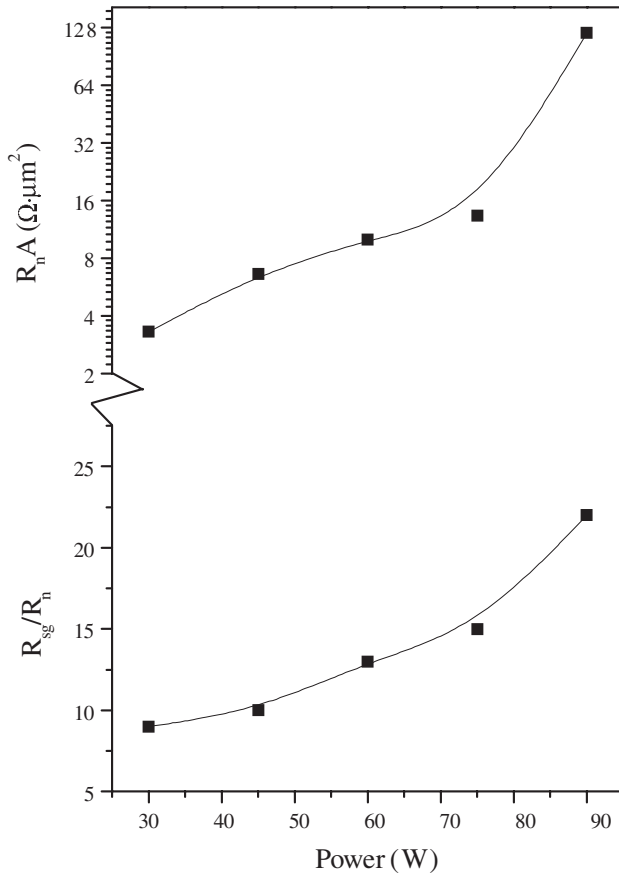
The layer thicknesses and sputtering conditions are listed in table 1. The voltage–current characteristics (VCC) of the junctions are measured in liquid helium and characterized by a software program developed by Ermakov *et al* [20]. The VCC are characterized on the basis of two key parameters: the specific junction resistance, $R_n A$ value, and the quality factor, R_{sg}/R_n (the ratio of sub-gap and normal resistances). We use the $R_n A$ value rather than the critical current density for junction characterization because this parameter is much easier and faster to measure. This circumstance is of great importance for us, since our research is based on the processing of a large amount of junctions. Moreover, the critical current density can be calculated from the gap voltage by the Ambegaokar–Baratoff relation [21].

3. Results and discussion

We explore the influence of nitrogen pressure, discharge power and nitridation time on junction properties. The investigation of the dependence of junction properties versus nitridation time has been carried out under a nitrogen pressure fixed at 50 mTorr and an applied power fixed at 30 W. These settings result in the following nitrogen ion flux parameters: $J_i = 0.22 \text{ A m}^{-2}$ and $V_{sh} = 21 \text{ V}$. Figure 3 illustrates the dependence of $R_n A$ and R_{sg}/R_n versus nitridation time. Both

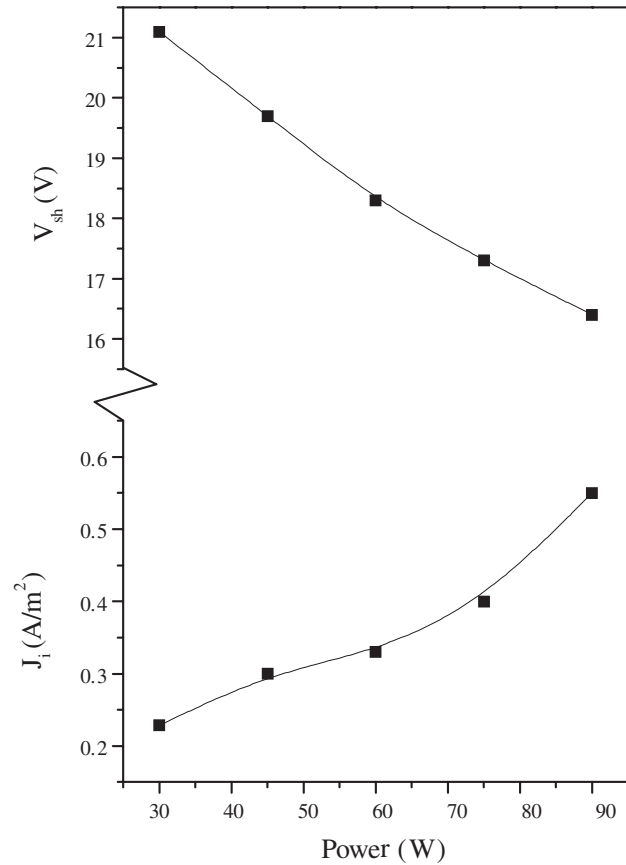
Table 1. Sputtering conditions of the layers used for SIS junction production.

Layer	Power (W)	Ar pressure (mTorr)	Deposition rate (nm min ⁻¹)	Thickness (nm)
Nb bottom electrode of SIS junction	300	8	100	300
Al layer	40	8	20	7
Nb top electrode of SIS junction	300	8	100	50
Nb top wiring	300	8	100	300
Au layer	100	8	180	50

**Figure 5.** Junction properties versus applied power. Nitrogen pressure is kept at 50 mTorr for all data points.

curves show a monotonic increase with time and a certain plateau at the beginning. Such a behaviour is due to the combination of two processes: nitridation of the Al layer and deposition of the AlN_x material. The deposition of AlN_x equals 6 \AA h^{-1} and is a monotonic process in time. However, nitridation of the Al layer reaches saturation, as has been shown by Bumble *et al* [10]. Park *et al* [22] have observed a similar behaviour for the Si nitridation process.

Variation of the nitrogen pressure, keeping the other parameters fixed (30 W applied power, 7 min nitridation time) does not result in a significant change in the $R_n A$ values. The tunnel barrier formation is almost exclusively determined by nitridation in this experiment, since the duration of the process is too short to result in a significant thickness of the deposited AlN_x material. All junctions, having tunnel barriers produced in the interval of 10–50 mTorr, have $R_n A = 4.4 \pm 1.5 \text{ } \Omega \mu m^2$ and $R_{sg}/R_n = 8.4 \pm 1.5$. The absence of any substantial changes in junction properties in this

**Figure 6.** Voltage drop across the substrate sheath and ion current density injected into the sheath. Nitrogen pressure is kept at 50 mTorr for all data points.

experiment is due to a moderate dependence of nitrogen ion flux on pressure (figure 4). The ion density slightly increases with pressure, while the sheath voltage slightly decreases with pressure.

An increase of the applied power, keeping the other parameters fixed (50 mTorr nitrogen pressure, 7 min nitridation time) results in an increase in $R_n A$ and R_{sg}/R_n values (figure 5). The deposited thickness of the AlN_x material is also negligible in this experiment, due to the short duration of the process. Nitrogen ion flux characteristics are illustrated in figure 6. The ion density considerably increases with an increase in applied power, while the sheath voltage shows a very moderate decrease.

Typical junction VCC are illustrated in figure 7. The critical current is suppressed by a magnetic field. As the current density increases the sub-gap leakage also increases, indicating that thinner tunnel barriers contain more defects.

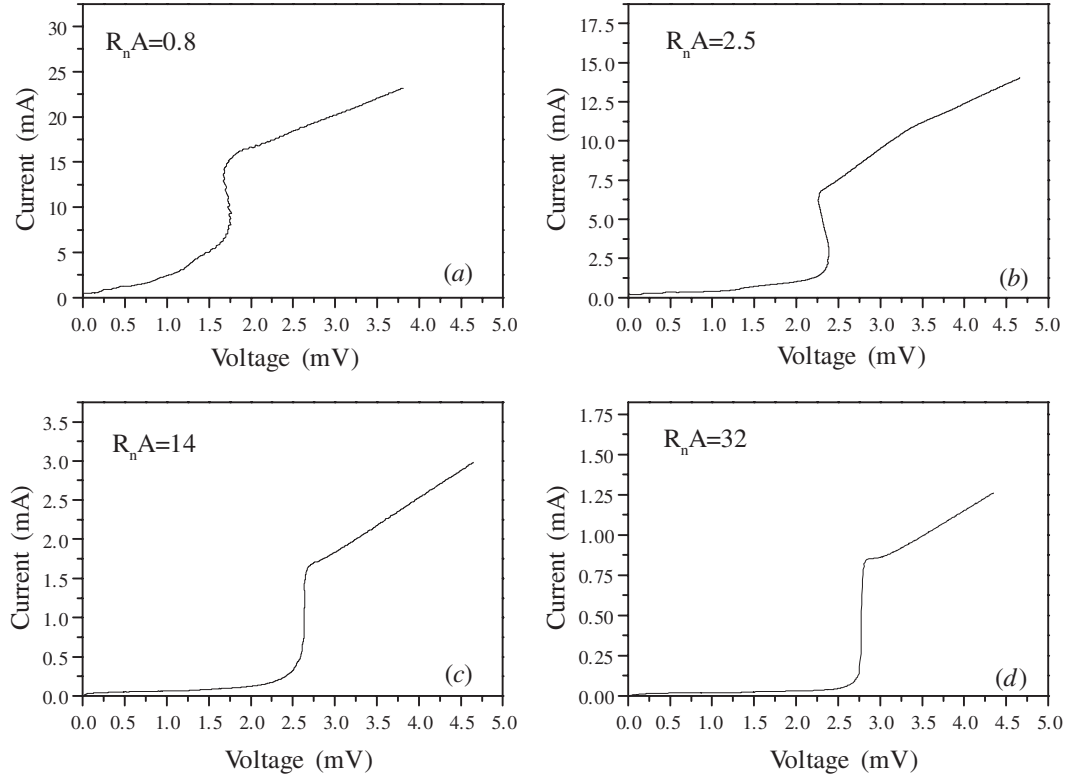


Figure 7. Typical VCC of SIS junctions with different $R_n A$ values. The size of all junctions is $10 \mu\text{m}^2$.

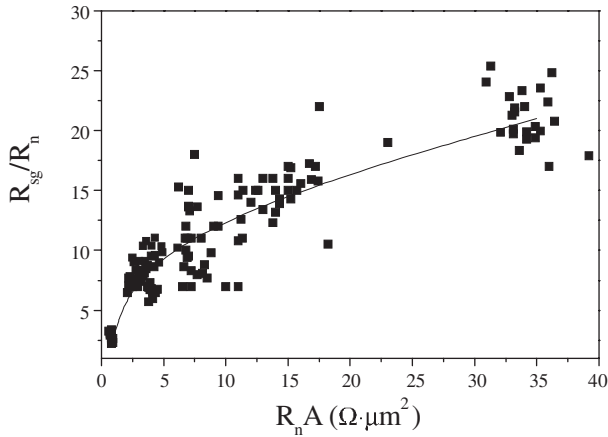


Figure 8. Junction quality parameter R_{sg}/R_n versus specific junction resistance $R_n A$.

The gap voltage is gradually reduced with an increase in $R_n A$ values due to self-heating of the junctions. The same phenomenon causes the back bending of the VCC at the gap voltage for the junctions with low $R_n A$ values. The bends of the VCC curve at 2.0 mV and 3.5 mV in figures 7(a) and (b) correspondingly is due to the transition of the junction wiring to the normal state. Figure 8 illustrates the dependence of R_{sg}/R_n versus $R_n A$ in the interval of 0–40 $\Omega \mu\text{m}^2$ for all junctions produced in these experiments. It is interesting to note that despite the different conditions of the tunnel barrier formation there is a well-defined correlation between the junction quality and $R_n A$ value.

The nitrogen ion flux, bombarding the Al surface, consists mainly of N_2^+ ions and a small fraction of N^+ ions of the

order of a few per cent [23]. N_2^+ ions undergo dissociation on the substrate surface with equal splitting of the retaining energy between nitrogen atoms due to the so-called ‘shrapnel effect’ [24]. If we take into account that the initial energy of N_2^+ ions in our system does not exceed 21 eV and the dissociation energy of nitrogen is 9.7 eV, then the energy of nitrogen atoms on the surface in this process will be about a few eV, which is clearly insufficient for implantation into the Al layer [25]. In contrast, N^+ ions with the energy of 20 eV, according to the SRIM program simulation, have almost zero reflection coefficient and a projected range of 5 Å into the Al layer and 6 Å into the AlN layer [26]. The channelling effects are not taken into account, because the texture of a thin Al layer on a rough Nb surface is very broad and therefore this effect may affect a very small fraction of Al grains [27, 28]. If we assume that the ion flux contains 1% of N^+ ions, then the density of implanted nitrogen atoms will equalize with the density of Al atoms on the (111) plane in 7 min in the experiment with nitridation time variation (figure 3). Since this time interval is of the same order of magnitude as the duration of the tunnel barrier formation, and the tunnel barrier itself consists of a few monolayers of AlN_x, it is concluded that the flux of atomic nitrogen ions is a major initial factor in tunnel barrier formation. On the other hand, the projected range of implanted nitrogen atoms is about two times lower compared to the typical tunnel barrier thickness [29]. This is a clear indication that nitrogen diffusion in Al and/or in AlN_x facilitated by plasma heating is a finalizing process in tunnel barrier formation. The presence of a diffusive component in this process is well recognized in a number of theoretical and experimental works [30–32]. Thus a saturation of nitrided depth of the Al layer in time (figure 3) is due to

the fact that nitrogen, incorporated into the stoichiometric AlN layer, diffuses out under a strong temperature gradient on the substrate surface developed by plasma heating [22, 30–32]. Additional confirmation of the diffusive nature of AlN_x tunnel barrier formation can be drawn from the experiment with applied power variation. An increase in the tunnel barrier thickness in this experiment is due to an increase in power dissipated on a substrate surface, since V_{sh} is almost constant and J_i increases almost proportionally to the applied power (figure 6). It is interesting to make a remark about the energy budget of this system. The power density dissipated on the substrate, estimated as a product of J_i and V_{sh} , is less than 1% of the minimum power that has to be applied to the driven electrode for a sustaining of plasma (7 W). Therefore, there is a fundamental difference between the process of Al nitridation on the driven electrode and on the electrode parallel to the driven electrode.

4. Conclusions

We have developed and characterized a system for the production of high-quality Nb/Al–AlN_x/Nb tunnel junctions with low $R_n A$ values. The rf glow discharge in the atmosphere of nitrogen is employed for Al layer nitridation. Locating the substrate on the electrode parallel to the driven electrode allows us to achieve a very mild bombardment of the substrate surface by nitrogen ions accelerated by the plasma potential. The influence of various technological factors on junction properties has been examined. An increase in nitridation time results in an increase of junction resistance. An increase in AlN_x tunnel barrier thickness in this experiment is due to the processes of Al layer nitridation and deposition of the AlN_x material. Variation of nitrogen pressure, keeping the other parameters fixed, does not affect the junction properties, while an increase in applied power results in a sharp increase in junction resistance. Analysis of the experimental data led us to the conclusion that AlN_x tunnel barrier formation is a complex combination of nitrogen implantation and subsequent diffusion of nitrogen, facilitated by plasma heating. In addition, despite different conditions of tunnel barrier formation in different experiments, there is a unique dependence of sub-gap leakage current versus transitivity of the tunnel barrier.

Acknowledgments

The authors thank P C Zalm, V V Gann, G de Lange, V P Koshelets, E K Kov'ev, P N Dmitriev, H Romijn, E van de Drift, M Zuiddam and T Zijlstra for helpful discussions. The work was supported in parts by ESA contract 11653/95, INTAS project 01-0367, and the RFBR project 00-02-16270.

References

- [1] Bin M, Gaidis M C, Zamudzinis J, Phillips T G and LeDuc H G 1996 Low-noise 1 THz niobium superconducting tunnel junction mixer with a normal metal tuning circuit *Appl. Phys. Lett.* **68** 1714–6
- [2] Di Leo R, Nigro A, Nobile G and Vaglio R 1990 Niobium–titanium nitride thin films for superconducting rf accelerator cavities *J. Low Temp. Phys.* **78** 41–50
- [3] Uzawa Y, Kawakami A, Miki S and Wang Z 2001 Performance of Al–NbN quasi-optical SIS mixers for the terahertz band *IEEE Trans. Appl. Supercond.* **11** 183–6
- [4] Yamamori H and Shoji A 1999 Improvement of uniformity of NbCN/MgO/NbCN Josephson junctions for large-scale circuit applications *Supercond. Sci. Technol.* **12** 877–9
- [5] Kawamura J, Chen J, Miller D, Kooi J, Zamudzinis J, Bumble B, LeDuc H G and Stern J A 1999 Low-noise submillimeter-wave NbTiN superconducting tunnel junction mixers *Appl. Phys. Lett.* **75** 4013–6
- [6] Jackson B D, Baryshev A M, de Lange G, Gao J R, Shitov S V, Iosad N N and Klapwijk T M 2001 Low-noise 1 THz superconductor–insulator–superconductor mixer incorporating a NbTiN/SiO₂/Al tuning circuit *Appl. Phys. Lett.* **79** 436–8
- [7] Iosad N N, Mijiritskii A V, Roddatis V V, van der Pers N M, Jackson B D, Gao J R, Polyakov S N, Dmitriev P N and Klapwijk T M 2000 Properties of (Nb_{0.35}Ti_{0.15})_xN_{1–x} thin films deposited on silicon wafers at ambient substrate temperature *J. Appl. Phys.* **88** 5756–9
- [8] Iosad N N, Jackson B D, Klapwijk T M, Polyakov S N, Dmitriev P N and Gao J R 1999 Optimization of RF- and DC-sputtered NbTiN films for integration with Nb-based SIS junctions *IEEE Trans. Appl. Supercond.* **9** 1716–9
- [9] Iosad N N, Jackson B D, Ferro F, Gao J R, Polyakov S N, Dmitriev P N and Klapwijk T M 1999 Source optimization for magnetron sputter-deposition of NbTiN tuning elements for SIS THz detectors *Supercond. Sci. Technol.* **12** 736
- [10] Bumble B, LeDuc H G, Stern J A and Megerian K G 2001 Fabrication of Nb/AlN_x/NbTiN junctions for SIS mixer applications *IEEE Trans. Appl. Supercond.* **11** 76–9
- [11] Klabunde K J 1985 *Thin Films from Free Atoms and Particles* (New York: Academic) p 113
- [12] Shiota T, Imamura T and Hasuo S 1992 Nb Josephson junction with an AlN_x barrier made by plasma nitridation *Appl. Phys. Lett.* **61** 1228–30
- [13] Dolata R, Neunhaus M and Jutzi W 1995 Tunnel barrier growth dynamics of Nb/AlO_x–Al/Nb and Nb/AlN_x–Al/Nb Josephson-junctions *Physica C* **241** 25–9
- [14] Kleinsasser A W, Mallison W H and Miller R E 1995 Nb/AlN/Nb Josephson-junctions with high critical-current density *IEEE Trans. Appl. Supercond.* **5** 2318–21
- [15] Smith D L 1995 *Thin Film Deposition* (New York: McGraw-Hill) p 406
- [16] Kohler K, Coburn J W, Horne D E, Kay E and Keller J H 1985 Plasma potentials of 13.56-MHz rf argon glow discharges in a planar system *J. Appl. Phys.* **57** 59–66
- [17] Logan J S 1970 Control of RF sputtered film properties through substrate tuning *IBM J. Res. Dev.* **14** 172–5
- [18] Keller J H and Pennebaker W B 1979 Electrical properties of RF sputtering systems *IBM J. Res. Dev.* **23** 3–15
- [19] Kroger H, Smith L N and Jillic D W 1981 Selective niobium anodization process for fabricating Josephson tunnel junctions *Appl. Phys. Lett.* **39** 280–2
- [20] Ermakov A B, Shitov S V, Baryshev A M, Koshelets V P and Luinge W 2001 A data acquisition system for test and control of superconducting integrated receivers *IEEE Trans. Appl. Supercond.* **11** 840
- [21] Ambegaokar V and Baratoff A 1963 Tunneling between superconductors *Phys. Rev. Lett.* **10** 486–91
- [22] Park K H, Kim B C and Kang H 1992 Silicon nitride formation by low energy N⁺ and N₂⁺ ion beams *J. Chem. Phys.* **97** 2742–9
- [23] Hultman L, Sundgren J-E, Greene J E, Bergstrom D B and Petrov I 1995 High-flux low-energy (similar-or-equal-to-20 eV) N₂⁺ ion irradiation during TiN deposition by reactive magnetron sputtering—effects on microstructure and preferred orientation *J. Appl. Phys.* **78** 5935
- [24] Klabunde K J 1985 *Thin Films from Free Atoms and Particles* (New York: Academic) p 211
- [25] Tzanev S, Golichovski A, Mix W and Showdon K J 1995 Scattering of fast N₂, N₂⁺, N₂²⁺, from Al(111) under glancing angles of incidence *Surf. Sci.* **331** 327–31

- [26] Ziegler J F, Biersack J P and Littmark U 1996 *The Stopping and Range of Ions in Solids* (New York: Pergamon)
- [27] Rodriguez-Navarro A B 2001 Model of texture development in polycrystalline films growing on amorphous substrates with different topographies *Thin Solid Films* **389** 288–95
- [28] Imamura T and Hasuo S 1991 Cross-sectional TEM observation of Nb/AlO_x–Al/Nb junction structures *IEEE Trans. Magn.* **27** 3172–75
- [29] Wang Z, Terai H, Kawakami A and Uzawa Y 1999 Interface and tunneling barrier heights of NbN/AlN/NbN tunnel junctions *Appl. Phys. Lett.* **75** 701–3
- [30] Harper J M E, Cuomo J J and Hentzell H T G 1985 Synthesis of compound thin films by dual ion beam deposition: I. Experimental approach *J. Appl. Phys.* **58** 550–5
- [31] Netterfield R P, Muller K-H, McKenzie D R, Goonan M J and Martin P J 1988 Growth dynamics of aluminum nitride and aluminium oxide thin films synthesized by ion-assisted deposition *J. Appl. Phys.* **63** 760–9
- [32] Wang X, Charlamov V, Koltisch A, Posselt M, Trushin Y and Moller W 1998 Study of ion beam assisted deposition of Al/AlN multilayers by comparison of computer simulation and experiment *J. Phys. D: Appl. Phys.* **31** 2241–4